

Nuclear modification factor in Pb-Pb and p-Pb collisions using Boltzmann transport equation

Liyun Qiao, Guorong Che, Jinbiao Gu, Hua Zheng and
Wenchao Zhang

School of Physics and Information Technology, Shaanxi Normal University, Xi'an
710119, People's Republic of China

E-mail: wenchao.zhang@snnu.edu.cn

Abstract.

We investigate the nuclear modification factor (R_{AA}) of identified particles as a function of transverse momentum (p_T) in Pb-Pb collisions at $\sqrt{s_{NN}} = 2.76$ and 5.02 TeV, as well as p-Pb collision at 5.02 TeV in the framework of Boltzmann transport equation with relaxation time approximation. In this framework, the initial distribution of particles is chosen as the Tsallis distribution and the local equilibrium distribution as the Boltzmann-Gibbs blast-wave distribution. The non-extensive parameter q_{pp} , the Tsallis temperature T_{pp} and the equilibrium temperature T_{eq} are set to be in common for all particles, while the ratio of kinetic freeze-out time to relaxation time t_f/τ is different for different particles when we performed a combined fit to the R_{AA} spectra of different particles at a given centrality. We observe that the fitted curves describe the spectra well up to $p_T \approx 3$ GeV/c. q_{pp} and T_{eq} (t_f/τ) decrease (increases) with centrality nonlinearly, while T_{pp} is almost independent of centrality. The dependence of the rate at which q_{pp} , T_{eq} or t_f/τ changes with centrality on the energy and the size of the colliding system is discussed.

PACS numbers: 25.75.Dw, 25.75.Nq, 24.10.Nz, 13.85.Ni

1. Introduction

Quantum-Chromodynamics (QCD) predicts that at high temperature and energy density there exists a hot and dense strongly interacting matter. This matter is commonly denoted as quark-gluon plasma (QGP), where partons (quarks and gluons) are the dominant degrees of freedom [1]. QGP is expected to be produced in ultra-relativistic heavy-ion collisions. As the partons propagate through QGP, they lose energy due to gluon emission and parton splitting[‡] [2]. Understanding the mechanism of parton energy loss is thus one of the main goals in heavy-ion collisions. The energy loss can be investigated via the study of the difference of the transverse momentum (p_T) spectrum in heavy-ion collisions compared to that in proton-proton (pp) collisions at the same energy. The difference is quantified by the nuclear modification factor $R_{AA(pA)}$, which is defined as [3, 4]

$$R_{AA(pA)}(p_T) = \frac{1}{\langle N_{\text{coll}} \rangle} \frac{(1/2\pi p_T) d^2 N_{AA(pA)} / dy dp_T}{(1/2\pi p_T) d^2 N_{pp} / dy dp_T}, \quad (1)$$

where $(1/2\pi p_T) d^2 N_{AA(pA)} / dy dp_T$ is the invariant p_T spectrum of nucleus-nucleus (AA) or proton-nucleus (pA) collisions, $(1/2\pi p_T) d^2 N_{pp} / dy dp_T$ is the invariant p_T spectrum in pp collisions. $\langle N_{\text{coll}} \rangle$ is the average number of binary nucleon-nucleon collisions at a given centrality and is estimated by the Glauber model of the nuclear collision geometry [5]. In the absence of nuclear modification, $R_{AA(pA)}$ equals to unity. An observation of $R_{AA(pA)}$ deviating from 1 indicates the presence of in-medium effects.

As shown in refs. [6, 7, 8], the nuclear modification factor can also be expressed as

$$R_{AA(pA)} = \frac{f_{fin}}{f_{in}}, \quad (2)$$

where f_{in} refers to the p_T distribution of particles produced immediately after collisions and f_{fin} refers to the final p_T distribution of particles. f_{fin} can be obtained by plugging the initial distribution f_{in} and the local equilibrium distribution f_{eq} into Boltzmann transport equation (BTE) with relaxation time approximation (RTA) [9]. In ref. [7], f_{in} was chosen as the Tsallis distribution [10] and f_{eq} as the Boltzmann-Gibbs distribution. The expression in equation (2) then was fitted individually to the R_{AA} spectra of pions, kaons, protons, K_S^0 , Λ , D^0 and J/ψ (π^0 and D^0) in the most central Pb-Pb (Au-Au) collisions at $\sqrt{s_{NN}} = 2.76$ TeV (200 GeV). For the heavy flavour hadrons, equation (2) can describe the R_{AA} spectra well. However, for the light flavour hadrons, it can only explain the R_{AA} spectra in the intermediate to high p_T region. In ref. [8], the authors took f_{eq} as the Boltzmann-Gibbs blast-wave (BGBW) function [11]. They performed an individual fit to the R_{AA} spectrum of pions, kaons, protons, K^{*0} or ϕ in the most central Pb-Pb collisions at $\sqrt{s_{NN}} = 2.76$ TeV. It was observed that the R_{AA} spectra of pions, kaons, K^{*0} and ϕ can be well described, while not for protons.

In this paper, as a complementary study to that conducted in refs. [7, 8], we investigate the R_{AA} spectra of identified particles not only at the most central but also

[‡] In the paper, we focus on low momentum particles that originate from the QGP. Jet quenching effects are beyond the scope of this work.

at the non-central Pb-Pb collisions at $\sqrt{s_{\text{NN}}} = 2.76$ TeV in the framework of BTE with RTA. Similarly as done in ref. [8], we set f_{in} as the Tsallis distribution and f_{eq} as the BGBW distribution. At a given centrality, we perform a combined rather than an individual fit on the R_{AA} spectra of identified particles. In the combined fit, the following parameters are set to be in common for all particles: the non-extensive parameter q_{pp} , the Tsallis temperature T_{pp} , the equilibrium temperature T_{eq} , the average transverse velocity $\langle\beta\rangle$ and the exponent of the transverse velocity profile n . Another parameter is the ratio of kinetic freeze-out time to relaxation time t_f/τ , which is different for different particles. We then extend our investigation to the R_{AA} ($R_{p\text{Pb}}$) spectra of identified particles at different centralities in Pb-Pb (p-Pb) collisions at 5.02 TeV. The combined fit can provide insight on the degree of deviation from equilibrium for the system produced immediately after collisions, the temperature of the system at the local equilibrium and the time taken by the system to reach the equilibrium. Its usefulness lies in the ability to compare the results at different energies in the same colliding system and the results in different colliding systems at the same energy. From our study, we observe that the model can describe the R_{AA} or $R_{p\text{Pb}}$ spectra of identified particles up to 3 GeV/c. Additionally, T_{eq} and q_{pp} (t_f/τ) decrease (increases) with centrality, while T_{pp} is almost independent of centrality. The rate at which T_{eq} , q_{pp} or t_f/τ changes with centrality depends on the energy and the size of the colliding system.

The organization of this paper is as follows. In section 2, we briefly describe the derivation of the nuclear modification factor in the framework of BTE with RTA. In section 3, we present the results of the combined fit to the R_{AA} ($R_{p\text{Pb}}$) spectra of identified particles in Pb-Pb (p-Pb) collisions at 2.76 and 5.02 (5.02) TeV and make some discussions. Finally, the conclusion is given in section 4.

2. Nuclear modification factor in the framework of BTE with RTA

The derivation of the nuclear modification factor in the framework of BTE with RTA is described explicitly in refs. [7, 8]. Here we only show the result,

$$R_{AA(pA)} = \frac{f_{eq}}{f_{in}} + \left(1 - \frac{f_{eq}}{f_{in}}\right) e^{-\frac{t_f}{\tau}}, \quad (3)$$

where t_f is the kinetic freeze-out time, τ is the relaxation time characterizing the time scale for the non-equilibrium system to relax to the local equilibrium. f_{in} (f_{eq} , f_{fin}) is the particle distribution at $t = 0$ (τ , t_f).

As described in ref. [12], the system produced immediately after the high energy collisions usually stays away from thermal equilibrium. The temperature of the system T_B fluctuates from event to event. Such a situation is described by a non-extensive statistics, i.e., the Tsallis statistics [10]. Therefore, as done in ref. [8], we set the initial

§ In the combined fit, $\langle\beta\rangle$ and n are respectively fixed to values returned from a combined blast-wave fit on the pion, kaon and proton p_T spectra at the given centrality. See the explanation in section 3.

distribution as the thermodynamically consistent Tsallis distribution [14]

$$f_{in} = C_{in} m_T \left[1 + (q_{pp} - 1) \frac{p_T}{T_{pp}} \right]^{-\frac{q_{pp}}{q_{pp}-1}}, \quad (4)$$

where m_T is the transverse mass, $C_{in} = gV/(2\pi)^2$, g is the degeneracy factor, V is the volume of the system. T_{pp} is the Tsallis temperature, whose reciprocal represents the average value of $1/T_B$. q_{pp} is the non-extensive parameter, which is connected to the variance of $1/T_B$ [13]. It measures the degree of deviation from equilibrium. The Tsallis distribution has been extensively used for the study of particle distributions in pp collisions [14, 15, 16, 17, 18, 19] and also in heavy ion collisions [20, 21, 22, 23, 24].

Once reaching the local equilibrium at the time $t = \tau$, the system will undergo the hydrodynamic evolution and finally freeze-out at the time $t = t_f$. Thus, as done in ref. [8], we take the local equilibrium distribution as the BGBW function [11],

$$f_{eq} = C_{eq} m_T \int_0^{R_0} r dr K_1(\xi_m) I_0(\xi_p), \quad (5)$$

where $C_{eq} = 2g\tau/(2\pi)^2$, $K_1(\xi_m)$ ($I_0(\xi_p)$) is the modified Bessel function of the second (first) kind. $\xi_m = m_T \cosh \rho / T_{eq}$, $\xi_p = p_T \sinh \rho / T_{eq}$, T_{eq} is the equilibrium temperature, $\rho = \tanh^{-1}(\beta_s(r/R_0)^n)$ is the transverse rapidity, r is the radial distance, β_s is the transverse flow velocity at the fireball surface ($r = R_0$), n is the exponent of the velocity profile. The average transverse velocity is $\langle \beta \rangle = 2/(n+2)\beta_s$. With the substitution of equations (4) and (5) into equation (3), the nuclear modification factor is written as

$$R_{AA(pA)} = \frac{C_{eq} \int_0^{R_0} r dr K_1(\xi_m) I_0(\xi_p)}{C_{in} \left[1 + (q_{pp} - 1) \frac{p_T}{T_{pp}} \right]^{-\frac{q_{pp}}{q_{pp}-1}}} + \left(1 - \frac{C_{eq} \int_0^{R_0} r dr K_1(\xi_m) I_0(\xi_p)}{C_{in} \left[1 + (q_{pp} - 1) \frac{p_T}{T_{pp}} \right]^{-\frac{q_{pp}}{q_{pp}-1}}} \right) e^{-\frac{t_f}{\tau}}. \quad (6)$$

The above expression incorporates a picture that particles produced in pp collisions undergo the evolution with a kinetic theory of BTE in RTA.

3. Results and discussions

The ALICE collaboration have published the R_{AA} spectra of pions, kaons and protons (the resonances K^{*0} and ϕ) at 0-5%, 5-10%, 10-20%, 20-40%, 40-60% and 60-80% (0-5%, 5-10%, 20-30% and 40-50%) centralities in Pb-Pb collisions at 2.76 TeV in refs. [25, 26]. Here, the pion, kaon, proton and K^{*0} spectra respectively refer to the spectra of $\pi^+ + \pi^-$, $K^+ + K^-$, $p + \bar{p}$ and $K^{*0} + \bar{K}^{*0}$. For the Λ R_{AA} spectra, no official data are released so far. However, the ALICE collaboration have presented the Λ p_T spectra at 0-5%, 5-10%, 10-20%, 20-40%, 40-60% and 60-80% centralities in Pb-Pb collisions at this energy [27]. Moreover, the preliminary result of the Λ p_T spectra in pp collisions at 2.76 TeV is available [28]. Thus the Λ R_{AA} spectra at these centralities can be constructed using

equation (1). The values of $\langle N_{\text{coll}} \rangle$ in the denominator of this equation are taken from ref. [29]. Recently, the ALICE collaboration have also published the R_{AA} spectra of pions, kaons and protons at 0-5%, 5-10%, 10-20%, 20-40%, 40-60% and 60-80% centralities in Pb-Pb collisions at 5.02 TeV [30]. The R_{AA} spectra of Ξ and Ω (K^{*0} , ϕ , Λ , Ξ and Ω) in Pb-Pb collisions at 2.76 (5.02) TeV are not considered in this work, as they are not available so far.

As the system size and number of particles produced in pA collisions are between those in pp and AA collisions, the results in pA collisions have frequently been utilized as a reference to understand those in AA collisions. In ref. [31], the ALICE collaboration have published the p_T spectra of pions, kaons and protons at 0-5%, 5-10%, 10-20%, 20-40%, 40-60% and 60-80% centralities p-Pb collisions at 5.02 TeV. Moreover, they also presented the p_T spectra of these particles in pp collisions at this energy. Therefore, the R_{pPb} spectra at these centralities can be constructed using equation (1). The $\langle N_{\text{coll}} \rangle$ values are taken from ref. [32]. The ALICE collaboration have also published the p_T spectra of K^{*0} , ϕ , Λ , Ξ and Ω at different centralities in p-Pb collisions at 5.02 TeV [33, 34, 35]. However, the p_T spectra of these particles in pp collisions at this energy are not available so far. Therefore, in this work we do not consider their R_{pPb} spectra.

We first perform a combined fit on the R_{AA} spectra of pions, kaons, protons, Λ , K^{*0} and ϕ at the 0-5% centrality in Pb-Pb collisions at 2.76 TeV with equation (6) adopting a least χ^2 method. At high p_T , as a hard contribution may set in, the spectra are not expected to be described by the blast-wave model [36]. Therefore, we limit the combined fit to $p_T < 3 \text{ GeV}/c$. At low p_T , there is a large contribution from resonance decays for pions. In order to remove this contribution, we set the lower bound of the pion spectrum as $0.5 \text{ GeV}/c$, which is utilized by the experimental groups. In the fit, the statistical and systematic errors of the data points have been added in quadrature. As shown in ref. [14], the authors have fitted the π^\pm , K^\pm , $p(\bar{p})$, K_S^0 , Λ and Ξ^- spectra produced in pp collisions at 0.9 TeV with the thermodynamically consistent Tsallis distribution individually. They found that for all hadrons the non-extensive parameter was around 1.11 and the Tsallis temperature was around 70 MeV. Thus, in the combined fit, T_{pp} and q_{pp} are set to be in common for all particles. In ref. [36], in order to quantify the freeze-out parameters in Pb-Pb collisions at 2.76 TeV, a combined blast-wave fit of the pion, kaon and proton p_T spectra was performed. Similarly as done in that reference, we set the parameters T_{eq} , $\langle \beta \rangle$ and n for pions, kaons, protons, Λ , K^{*0} and ϕ in common in this work. As described in section 2, the system will reach the local equilibrium at $t = \tau$, then it will undergo the hydrodynamic evolution and finally freeze out at $t = t_f$. It is reasonable to assume that $\langle \beta \rangle$ and n at $t = \tau$ are respectively the same as those at $t = t_f$. Therefore, we fix $\langle \beta \rangle$ and n in f_{eq} respectively as 0.651 ± 0.020 and 0.712 ± 0.086 which were returned by the combined blast-wave fit of the pion, kaon and proton p_T spectra at the 0-5% centrality [36]. As the equilibration relies on the particle species and their interaction with the rest of the medium, the relaxation time differs from particles

|| In ref. [36], the upper limit for pions (kaons, protons) is 1 (1.5, 3) GeV/c. The parameters returned from the combined fit with these upper limits are consistent with those in the paper within errors.

to particles [7]. Thus we set t_f/τ to be different for different particles. As a result, there are nine parameters in the combined fit: three common parameters q_{pp} , T_{pp} and T_{eq} ; six parameters t_f/τ , one for each particle. They are listed in table 1. Also tabulated in the table is the χ^2 per degree of freedom (χ^2/dof)¶. The first uncertainty quoted in the table is returned from the combined fit. The second is determined by adding the errors returned from the variation of $\langle\beta\rangle$ and n in the combined fit respectively by $\pm 1\sigma$ in quadrature. The third is the uncertainty due to the variation of the lower fit bound (from 0.5 to 0.1 GeV/c) for pions. We then apply the same procedure to the R_{AA} spectra of pions, kaons, protons, Λ , K^{*0} and ϕ at the 5-10% centrality. For the 10-20%, 20-40%, 40-60% or 60-80% centrality, we can only perform a combined fit on the R_{AA} spectra of pions, kaons, protons and Λ , since the R_{AA} spectra of K^{*0} and ϕ at these centralities are not available so far. For the 20-30% or 40-50% centrality, we would like to perform a combined fit on the R_{AA} spectra of pions, kaons, protons, K^{*0} and ϕ . At these two centralities, the R_{AA} spectra of K^{*0} and ϕ have been published, but not the R_{AA} spectra of pions, kaons and protons. However, we can construct their R_{AA} spectra using equation (1), since their p_T spectra in Pb-Pb and pp collisions at 2.76 TeV are available in refs. [36, 37]. The parameters q_{pp} , T_{pp} , T_{eq} and t_f/τ at these centralities are also tabulated in table 1. The upper panels of figure 1 present the R_{AA} spectra together with the combined fit results at two selected centralities (0-5% and 60-80%). We observe that most of the data points appear consistent with the fitted curves which are described by equation (6). In order to address how much the combined fit is compatible with the data points statistically, a variable $\text{pull} = (\text{data} - \text{fitted})/\Delta\text{data}$ is evaluated. The pull distributions are presented in the lower panels of the figure. Except for the second point (the first and third points) in the kaon (ϕ) R_{AA} spectrum at the 0-5% centrality, we observe that all the other data points are consistent with the fitted curves within one standard deviation. In the region with $p_T > 3$ GeV/c (not shown in the figure), there is a large deviation between the data points and the fitted curve for the R_{AA} spectra of kaons and protons.

With the parameters in table 1, we show q_{pp} , T_{pp} , T_{eq} and t_f/τ versus centrality in figure 2. For q_{pp} , T_{eq} and t_f/τ , the dependence is clearly nonlinear and is parameterized with $a\langle N_{\text{part}}\rangle^b$, where a and b are free parameters, b represents the rate at which $\ln q_{pp}$, $\ln T_{eq}$ or $\ln t_f/\tau$ changes with $\ln\langle N_{\text{part}}\rangle$. $\langle N_{\text{part}}\rangle$ is the average value of the number of participants at a given centrality and is taken from ref. [29]. Several conclusions can be drawn from the results presented in the figure.

(i) q_{pp} decreases with centrality. The b value returned from the parameterization of q_{pp} is -0.030 ± 0.005 . It means that the initial distribution in central collisions remains closer to equilibrium than that in peripheral collisions.

(ii) T_{pp} at different centralities are consistent within errors. They are around 60.6 ± 3.3 MeV.

¶ The low χ^2/dof probably indicates the experimental systematic errors are strongly correlated and thus overestimated.

Table 1. Values of parameters from the combined fit to the R_{AA} spectra of identified particles at different centralities in Pb-Pb collisions at 2.76 TeV. The uncertainties are explained in the text.

	0 – 5%	5 – 10%
q_{pp}	$1.225 \pm 0.007 \pm 0.057 \pm 0.004$	$1.228 \pm 0.008 \pm 0.069 \pm 0.004$
T_{pp}	$0.058 \pm 0.009 \pm 0.045 \pm 0.010$	$0.062 \pm 0.010 \pm 0.054 \pm 0.009$
T_{eq}	$0.132 \pm 0.004 \pm 0.014 \pm 0.004$	$0.142 \pm 0.005 \pm 0.018 \pm 0.004$
$(t_f/\tau)_\pi$	$2.213 \pm 0.161 \pm 0.230 \pm 0.246$	$2.085 \pm 0.169 \pm 0.270 \pm 0.253$
$(t_f/\tau)_K$	$1.731 \pm 0.033 \pm 0.051 \pm 0.023$	$1.672 \pm 0.032 \pm 0.063 \pm 0.022$
$(t_f/\tau)_p$	$2.809 \pm 0.053 \pm 0.031 \pm 0.044$	$2.769 \pm 0.053 \pm 0.040 \pm 0.042$
$(t_f/\tau)_{K^*0}$	$2.526 \pm 0.134 \pm 0.019 \pm 0.016$	$2.199 \pm 0.121 \pm 0.017 \pm 0.009$
$(t_f/\tau)_\phi$	$1.574 \pm 0.074 \pm 0.001 \pm 0.008$	$1.508 \pm 0.073 \pm 0.001 \pm 0.010$
$(t_f/\tau)_\Lambda$	$2.118 \pm 0.106 \pm 0.024 \pm 0.026$	$2.038 \pm 0.103 \pm 0.029 \pm 0.024$
χ^2/dof	37.975/116	34.154/116
	10 – 20%	20 – 30%
q_{pp}	$1.226 \pm 0.007 \pm 0.064 \pm 0.005$	$1.236 \pm 0.009 \pm 0.068 \pm 0.014$
T_{pp}	$0.069 \pm 0.009 \pm 0.050 \pm 0.012$	$0.064 \pm 0.010 \pm 0.052 \pm 0.023$
T_{eq}	$0.151 \pm 0.004 \pm 0.017 \pm 0.004$	$0.163 \pm 0.005 \pm 0.017 \pm 0.005$
$(t_f/\tau)_\pi$	$2.107 \pm 0.179 \pm 0.297 \pm 0.328$	$1.955 \pm 0.180 \pm 0.265 \pm 0.387$
$(t_f/\tau)_K$	$1.601 \pm 0.028 \pm 0.062 \pm 0.029$	$1.476 \pm 0.029 \pm 0.060 \pm 0.048$
$(t_f/\tau)_p$	$2.682 \pm 0.050 \pm 0.043 \pm 0.053$	$2.507 \pm 0.050 \pm 0.041 \pm 0.076$
$(t_f/\tau)_{K^*0}$	—	$2.219 \pm 0.124 \pm 0.033 \pm 0.036$
$(t_f/\tau)_\phi$	—	$1.131 \pm 0.061 \pm 0.004 \pm 0.012$
$(t_f/\tau)_\Lambda$	$1.868 \pm 0.085 \pm 0.021 \pm 0.026$	—
χ^2/dof	22.329/108	17.608/99
	20 – 40%	40 – 50%
q_{pp}	$1.251 \pm 0.007 \pm 0.065 \pm 0.011$	$1.263 \pm 0.012 \pm 0.044 \pm 0.026$
T_{pp}	$0.054 \pm 0.009 \pm 0.048 \pm 0.018$	$0.062 \pm 0.013 \pm 0.038 \pm 0.037$
T_{eq}	$0.171 \pm 0.005 \pm 0.017 \pm 0.005$	$0.209 \pm 0.008 \pm 0.016 \pm 0.004$
$(t_f/\tau)_\pi$	$1.706 \pm 0.108 \pm 0.179 \pm 0.245$	$1.481 \pm 0.136 \pm 0.122 \pm 0.311$
$(t_f/\tau)_K$	$1.371 \pm 0.023 \pm 0.047 \pm 0.035$	$1.117 \pm 0.027 \pm 0.036 \pm 0.055$
$(t_f/\tau)_p$	$2.387 \pm 0.043 \pm 0.041 \pm 0.063$	$1.986 \pm 0.050 \pm 0.041 \pm 0.090$
$(t_f/\tau)_{K^*0}$	—	$1.540 \pm 0.107 \pm 0.026 \pm 0.036$
$(t_f/\tau)_\phi$	—	$0.811 \pm 0.056 \pm 0.007 \pm 0.012$
$(t_f/\tau)_\Lambda$	$1.599 \pm 0.072 \pm 0.022 \pm 0.026$	—
χ^2/dof	15.143/108	13.719/99
	40 – 60%	60 – 80%
q_{pp}	$1.267 \pm 0.010 \pm 0.045 \pm 0.028$	$1.342 \pm 0.026 \pm 0.039 \pm 0.022$
T_{pp}	$0.063 \pm 0.011 \pm 0.040 \pm 0.039$	$0.048 \pm 0.024 \pm 0.035 \pm 0.034$
T_{eq}	$0.219 \pm 0.008 \pm 0.018 \pm 0.004$	$0.344 \pm 0.028 \pm 0.025 \pm 0.003$
$(t_f/\tau)_\pi$	$1.378 \pm 0.109 \pm 0.122 \pm 0.302$	$0.851 \pm 0.073 \pm 0.041 \pm 0.149$
$(t_f/\tau)_K$	$1.023 \pm 0.022 \pm 0.036 \pm 0.054$	$0.658 \pm 0.021 \pm 0.016 \pm 0.026$
$(t_f/\tau)_p$	$1.843 \pm 0.042 \pm 0.045 \pm 0.091$	$1.180 \pm 0.044 \pm 0.034 \pm 0.058$
$(t_f/\tau)_\Lambda$	$1.149 \pm 0.062 \pm 0.011 \pm 0.027$	$0.780 \pm 0.066 \pm 0.017 \pm 0.033$
χ^2/dof	10.241/108	9.090/108

(iii) T_{eq} decreases with centrality. This trend is similar to that of the kinetic freeze-out temperature T_{kin} returned from the combined blast-wave fit on the pion, kaon and

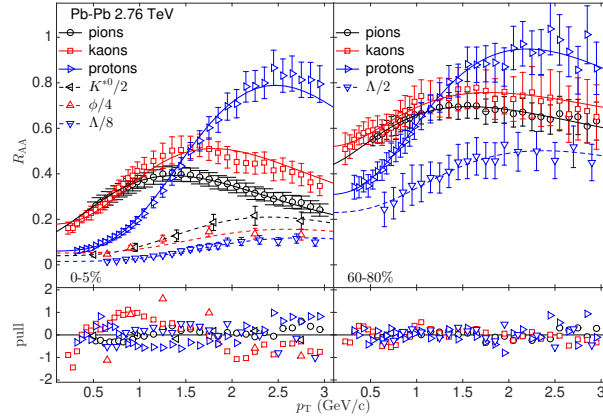


Figure 1. (Colour online) Top left (right) panel: the R_{AA} spectra of identified particles at the 0-5% (60-80%) centrality in Pb-Pb collisions at 2.76 TeV. The data points are taken from refs. [25, 26, 27, 28, 36, 37]. The curves represent the combined fit. Bottom left (right) panel: the pull distributions at the 0-5% (60-80%) centrality.

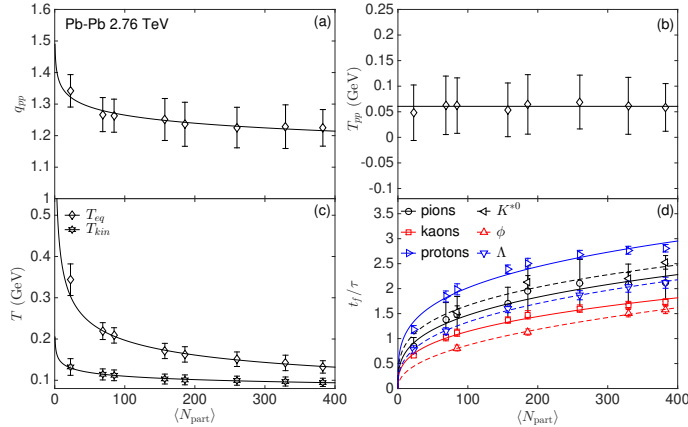


Figure 2. (Colour online) q_{pp} , T_{pp} , T_{eq} , T_{kin} and t_f/τ as a function of centrality in Pb-Pb collisions at 2.76 TeV. The error bar represents the total uncertainty of the parameter. Also shown in the figure is the parameterization of the dependence with $a\langle N_{part} \rangle^b$. The values of T_{kin} are taken from ref. [36].

proton p_T spectra in Pb-Pb collisions at 2.76 TeV [36]. At a given centrality, T_{eq} is larger than T_{kin} , which is consistent with the picture that the temperature decreases with the evolution of the system from the local equilibrium to the kinetic freeze-out. Moreover, the rate at which $\ln T_{eq}$ decreases with $\ln \langle N_{part} \rangle$ is 0.290 ± 0.012 , which is larger than that of $\ln T_{kin}$, 0.113 ± 0.007 .

(iv) t_f/τ increases with centrality. It means that the relaxation time τ in central collisions is less than that in peripheral collisions. As the initial distribution in central collisions is less off-equilibrium, the system will accordingly take less time to reach the local equilibrium. The b values for pions, kaons, protons, K^{*0} , ϕ and Λ are 0.318 ± 0.035 ,

0.334 ± 0.022 , 0.275 ± 0.033 , 0.287 ± 0.170 , 0.450 ± 0.044 and 0.356 ± 0.012 respectively. Moreover, at a given centrality, we observe that for mesons (baryons or resonances) t_f/τ is smaller for particles with heavier mass, which is in agreement with the conclusion in ref. [7].

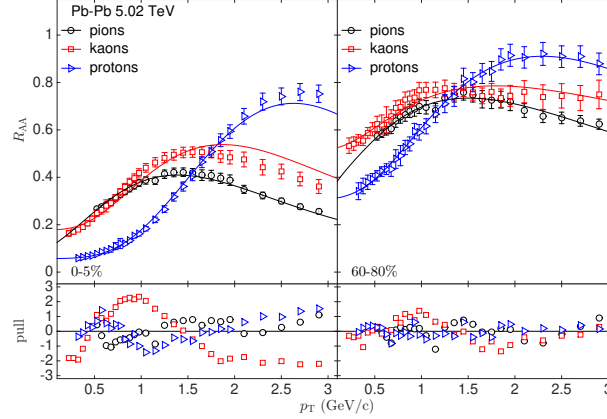


Figure 3. (Colour online) Top left (right) panel: the R_{AA} spectra of pions, kaons and protons at the 0-5% (60-80%) centrality in Pb-Pb collisions at 5.02 TeV. The data points are taken from ref. [30]. The curves represent the combined fit. Bottom left (right) panel: the pull distributions at the 0-5% (60-80%) centrality.

Next we investigate the R_{AA} spectra of pions, kaons and protons at the 0-5% centrality in Pb-Pb collisions at 5.02 TeV. We fix $\langle\beta\rangle$ and n respectively as 0.663 ± 0.003 and 0.735 ± 0.013 which were returned by a combined blast-wave fit of the pion, kaon and proton p_T spectra at this centrality in ref. [30]. Combined fits on the R_{AA} spectra at other centralities are performed similarly as that at the 0-5% centrality. In the upper panels of figure 3, we present the R_{AA} spectra together with the fit results at two selected centralities (0-5% and 60-80%). As can be seen from the pull distributions in the lower panels of the figure, at the 60-80% (0-5%) centrality most of the data points agree with the fitted curves within 1 (2) standard deviation(s). The parameters returned from the combined fits and their uncertainties are reported in table 2. Also listed in the table is the χ^2/dof^+ . The dependence of these parameters on centrality is shown in figure 4. In the figure, the values of $\langle N_{\text{part}} \rangle$ at different centralities are taken from ref. [38]. As can be seen from the figure, q_{pp} , T_{eq} , T_{kin} and t_f/τ rely nonlinearly on centrality. This trend is similar to that observed in Pb-Pb collisions at 2.76 TeV. Moreover, at a given centrality, we observe that q_{pp} , T_{eq} , T_{kin} , t_f/τ for pions, kaons and protons are respectively compatible with those at 2.76 TeV within errors. However, the rate at which $\ln q_{pp}$ ($\ln T_{eq}$, $\ln T_{kin}$) changes with $\ln \langle N_{\text{part}} \rangle$ is -0.022 ± 0.004 (-0.334 ± 0.018 , -0.140 ± 0.014), whose absolute value is smaller (larger, larger) than that at 2.76 TeV. This means at high energy q_{pp} (T_{eq} , T_{kin}) decreases slower (faster, faster) with centrality

⁺ The χ^2/dof increases with centrality, probably indicating the experimental uncertainties in peripheral collisions are more overestimated than in central collisions.

Table 2. Values of parameters from the combined fit to the pion, kaon and proton R_{AA} spectra at different centralities in Pb-Pb collisions at 5.02 TeV. T_{pp} and T_{eq} are in units of GeV. The uncertainties are the same as those in table 1.

	0 – 5%	5 – 10%	10 – 20%
q_{pp}	$1.229 \pm 0.011 \pm 0.008 \pm 0.001$	$1.2241 \pm 0.0095 \pm 0.0077 \pm 0.0002$	$1.234 \pm 0.011 \pm 0.007 \pm 0.002$
T_{pp}	$0.056 \pm 0.014 \pm 0.006 \pm 0.006$	$0.068 \pm 0.013 \pm 0.006 \pm 0.003$	$0.066 \pm 0.014 \pm 0.005 \pm 0.008$
T_{eq}	$0.124 \pm 0.006 \pm 0.002 \pm 0.004$	$0.133 \pm 0.005 \pm 0.002 \pm 0.003$	$0.144 \pm 0.006 \pm 0.002 \pm 0.004$
$(t_f/\tau)_\pi$	$2.332 \pm 0.313 \pm 0.051 \pm 0.295$	$2.496 \pm 0.390 \pm 0.061 \pm 0.305$	$2.385 \pm 0.390 \pm 0.051 \pm 0.389$
$(t_f/\tau)_K$	$1.729 \pm 0.040 \pm 0.007 \pm 0.014$	$1.731 \pm 0.040 \pm 0.007 \pm 0.010$	$1.652 \pm 0.043 \pm 0.007 \pm 0.022$
$(t_f/\tau)_p$	$2.8623 \pm 0.0663 \pm 0.0005 \pm 0.0272$	$2.8156 \pm 0.0578 \pm 0.0005 \pm 0.0183$	$2.718 \pm 0.063 \pm 0.001 \pm 0.036$
χ^2/dof	110.408/76	76.928/76	86.283/76
	20 – 40%	40 – 60%	60 – 80%
q_{pp}	$1.249 \pm 0.012 \pm 0.007 \pm 0.008$	$1.278 \pm 0.015 \pm 0.008 \pm 0.015$	$1.297 \pm 0.019 \pm 0.011 \pm 0.027$
T_{pp}	$0.066 \pm 0.015 \pm 0.005 \pm 0.018$	$0.073 \pm 0.018 \pm 0.006 \pm 0.037$	$0.103 \pm 0.026 \pm 0.009 \pm 0.085$
T_{eq}	$0.165 \pm 0.007 \pm 0.002 \pm 0.008$	$0.220 \pm 0.013 \pm 0.003 \pm 0.019$	$0.328 \pm 0.035 \pm 0.009 \pm 0.064$
$(t_f/\tau)_\pi$	$2.124 \pm 0.348 \pm 0.037 \pm 0.464$	$1.704 \pm 0.289 \pm 0.029 \pm 0.503$	$1.274 \pm 0.262 \pm 0.027 \pm 0.549$
$(t_f/\tau)_K$	$1.441 \pm 0.043 \pm 0.006 \pm 0.042$	$1.075 \pm 0.040 \pm 0.006 \pm 0.064$	$0.667 \pm 0.033 \pm 0.006 \pm 0.078$
$(t_f/\tau)_p$	$2.448 \pm 0.067 \pm 0.002 \pm 0.066$	$1.925 \pm 0.072 \pm 0.006 \pm 0.113$	$1.185 \pm 0.063 \pm 0.010 \pm 0.144$
χ^2/dof	104.950/76	68.931/76	24.874/76

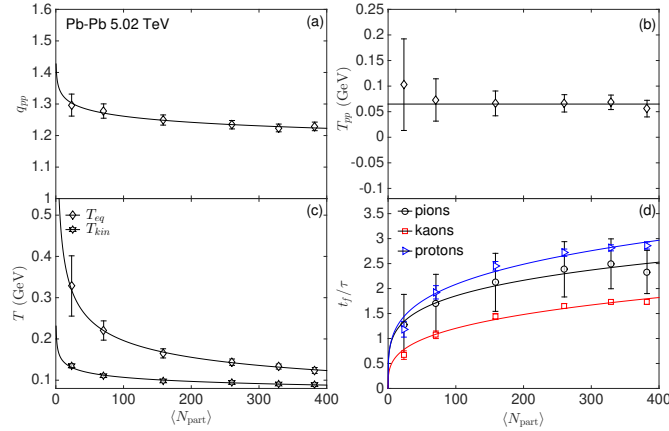


Figure 4. (Colour online) q_{pp} , T_{pp} , T_{eq} , T_{kin} and t_f/τ as a function of centrality in Pb-Pb collisions at 5.02 TeV. The error bar represents the total uncertainty of the parameter. Also shown in the figure is the parameterization of the dependence with $a\langle N_{\text{part}} \rangle^b$. The values of T_{kin} are taken from ref. [30].

than that at low energy in the same colliding system. For pions (kaons, protons), the rate at which $\ln t_f/\tau$ increases with $\ln \langle N_{\text{part}} \rangle$ is 0.224 ± 0.052 (0.298 ± 0.056 , 0.255 ± 0.049), which is smaller than (compatible with, compatible with) that at 2.76 TeV. For T_{pp} , it fluctuates around 64.8 ± 3.7 MeV, which is consistent with that at 2.76 TeV within errors. The conclusion that at a given centrality t_f/τ is smaller for particles with heavier mass also holds for mesons (pions and kaons) in Pb-Pb collisions at 5.02 TeV.

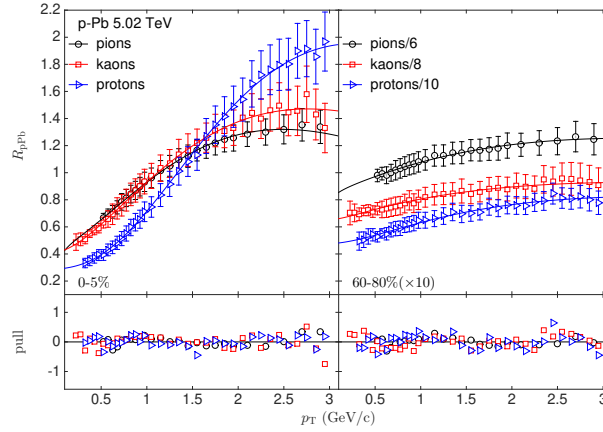


Figure 5. (Colour online) Top left (right) panel: the R_{pPb} spectra of pions, kaons and protons at the 0-5% (60-80%) centrality in p-Pb collisions at 5.02 TeV. The data points are taken from ref. [31]. The curves represent the combined fit. Bottom left (right) panel: the pull distributions at the 0-5% (60-80%) centrality.

Finally, we extend the investigation to the R_{pPb} spectra of pions, kaons and protons at a given centrality in p-Pb collisions at 5.02 TeV. In the combined fit, $\langle\beta\rangle$ and n are fixed as the corresponding values that were returned by a combined blast-wave fit of the pion, kaon, proton, K_S^0 and Λ p_T spectra at this centrality in ref. [34]. The combined fit results on the R_{pPb} at two selected centralities (0-5% and 60-80%) are presented in the upper panels of figure 5. From the lower panels of the figure, we observe that the data points are compatible with the fitted curves within 1 standard deviation at both centralities. The parameters returned from the combined fit and their uncertainties are listed in table 3. The dependence of these parameters on centrality is shown in figure 6. In the figure, the values of $\langle N_{part} \rangle$ at different centralities are taken from ref. [32]. The error bars of q_{pp} , T_{pp} and T_{eq} at the 60-80% centrality are relatively large. The main contributions to these error bars are the uncertainties returned from the fit and from the variation of the lower fit bound for pions. As can be seen from the figure, the dependence of q_{pp} , T_{eq} , T_{kin} and t_f/τ on centrality is nonlinear, which is similar to that in Pb-Pb collisions at 5.02 TeV. However, the rate at which $\ln q_{pp}$ ($\ln T_{eq}$, $\ln T_{kin}$) changes with $\ln \langle N_{part} \rangle$ is -0.154 ± 0.086 (-0.980 ± 0.283 , -0.148 ± 0.025), whose absolute value is larger than (larger than, compatible with) that in Pb-Pb collisions at 5.02 TeV. Thus, in the small system q_{pp} and T_{eq} (T_{kin}) decrease(s) with centrality faster than (at the similar rate as) those (that) in the large system at the same energy. For pions (kaons, protons), the rate at which $\ln t_f/\tau$ increases with $\ln \langle N_{part} \rangle$ is 0.846 ± 0.160 (0.380 ± 0.120 , 0.468 ± 0.100), which is larger than (compatible with, larger than) that in Pb-Pb collisions at 5.02 TeV. For T_{pp} , it fluctuates around 152.8 ± 10.4 MeV, which is larger than that in Pb-Pb collisions at 5.02 TeV. Moreover, for mesons, at a given centrality t_f/τ is smaller for heavy particles (kaons) than that for light particles (pions), which is consistent with the conclusions drawn in Pb-Pb collisions at 2.76 and 5.02 TeV.

Table 3. Values of parameters from the combined fit to the pion, kaon and proton R_{pPb} spectra at different centralities in p-Pb collisions at 5.02 TeV. T_{pp} and T_{eq} are in units of GeV. The uncertainties are the same as those in table 1.

	0 – 5%	5 – 10%	10 – 20%
q_{pp}	$1.213 \pm 0.011 \pm 0.021 \pm 0.153$	$1.218 \pm 0.014 \pm 0.036 \pm 0.163$	$1.204 \pm 0.013 \pm 0.033 \pm 0.191$
T_{pp}	$0.140 \pm 0.008 \pm 0.013 \pm 0.118$	$0.146 \pm 0.010 \pm 0.027 \pm 0.124$	$0.159 \pm 0.009 \pm 0.024 \pm 0.141$
T_{eq}	$0.309 \pm 0.015 \pm 0.009 \pm 0.177$	$0.341 \pm 0.022 \pm 0.018 \pm 0.210$	$0.337 \pm 0.023 \pm 0.020 \pm 0.257$
$(t_f/\tau)_\pi$	$1.980 \pm 0.502 \pm 0.159 \pm 1.336$	$1.937 \pm 0.506 \pm 0.358 \pm 1.220$	$2.454 \pm 0.935 \pm 0.518 \pm 1.697$
$(t_f/\tau)_K$	$0.948 \pm 0.041 \pm 0.030 \pm 0.267$	$1.011 \pm 0.047 \pm 0.063 \pm 0.259$	$1.060 \pm 0.046 \pm 0.056 \pm 0.280$
$(t_f/\tau)_p$	$1.271 \pm 0.024 \pm 0.014 \pm 0.144$	$1.303 \pm 0.030 \pm 0.031 \pm 0.159$	$1.295 \pm 0.028 \pm 0.026 \pm 0.167$
χ^2/dof	3.281/86	4.585/86	4.280/86
	20 – 40%	40 – 60%	60 – 80%
q_{pp}	$1.240 \pm 0.019 \pm 0.030 \pm 0.191$	$1.290 \pm 0.060 \pm 0.028 \pm 0.148$	$1.949 \pm 0.509 \pm 0.018 \pm 0.441$
T_{pp}	$0.160 \pm 0.011 \pm 0.020 \pm 0.144$	$0.188 \pm 0.026 \pm 0.017 \pm 0.170$	$0.119 \pm 0.250 \pm 0.009 \pm 0.205$
T_{eq}	$0.448 \pm 0.040 \pm 0.022 \pm 0.272$	$0.628 \pm 0.127 \pm 0.043 \pm 0.113$	$2.392 \pm 1.214 \pm 0.062 \pm 0.957$
$(t_f/\tau)_\pi$	$1.411 \pm 0.186 \pm 0.101 \pm 0.652$	$1.181 \pm 0.223 \pm 0.051 \pm 0.487$	$0.760 \pm 0.138 \pm 0.006 \pm 0.303$
$(t_f/\tau)_K$	$0.982 \pm 0.034 \pm 0.031 \pm 0.200$	$0.866 \pm 0.049 \pm 0.017 \pm 0.166$	$0.661 \pm 0.060 \pm 0.002 \pm 0.087$
$(t_f/\tau)_p$	$1.203 \pm 0.025 \pm 0.019 \pm 0.147$	$1.029 \pm 0.036 \pm 0.014 \pm 0.158$	$0.752 \pm 0.057 \pm 0.002 \pm 0.065$
χ^2/dof	2.880/86	4.178/86	3.717/86

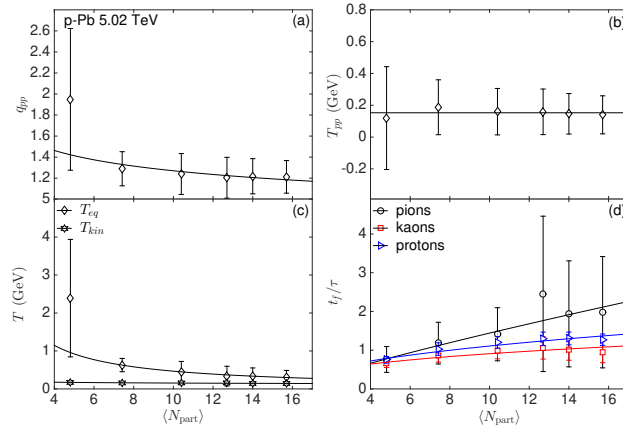


Figure 6. (Colour online) q_{pp} , T_{pp} , T_{eq} , T_{kin} and t_f/τ as a function of centrality in p-Pb collisions at 5.02 TeV. The error bar represents the total uncertainty of the parameter. Also shown in the figure is the parameterization of the dependence with $a\langle N_{part} \rangle^b$. The values of T_{kin} are taken from ref. [34].

4. Conclusions

In this paper, we have investigated the R_{AA} (R_{pPb}) spectra of identified particles at different centralities in Pb-Pb (p-Pb) collisions at 2.76 and 5.02 (5.02) TeV in the framework of BTE with RTA. In this framework, f_{in} is set to be the Tsallis distribution and f_{eq} to be the BGBW distribution. At a given centrality, a combined fit is performed on the spectra of identified particles with a least χ^2 method. In the combined fit, q_{pp} ,

T_{pp} and T_{eq} are set to be in common for all particles, while t_f/τ is different for different particles. We observe the fitted curves can describe the R_{AA} or R_{pPb} spectra well up to $p_T \approx 3$ GeV/c. q_{pp} and T_{eq} (t_f/τ) decrease (increases) with centrality nonlinearly. In the same colliding system, at high energy q_{pp} (T_{eq}) decreases slower (faster), while t_f/τ does not increase faster with centrality than that at low energy. At the same energy, in the large system q_{pp} (T_{eq}) decrease slower (slower), while t_f/τ does not increase faster with centrality than that in the small system. T_{pp} is almost independent of centrality, fluctuating around 60.6 ± 3.3 and 64.8 ± 3.7 (152.8 ± 10.4) MeV in Pb-Pb (p-Pb) collisions at 2.76 and 5.02 (5.02) TeV.

Acknowledgements

This work is supported by the Fundamental Research Funds for the Central Universities of China under GK201903022 and GK202003019, by the Scientific Research Foundation for the Returned Overseas Chinese Scholars, State Education Ministry, by Natural Science Basic Research Plan in Shaanxi Province of China (program No. 2020JM-289) and by the National Natural Science Foundation of China under Grant Nos. 11447024 and 11505108.

References

- [1] Shuryak E V 1980 Phys. Rept. **61** 71
- [2] Qin G Y et al 2015 Int. J. Mod. Phys. E **24** 1530014
- [3] Khachatryan V *et al* (CMS Collaboration) 2017 JHEP **04** 039
- [4] Adam J *et al* (ALICE Collaboration) 2015 Phys. Rev. C **91** 064905
- [5] Miller M L *et al* 2007 Ann. Rev. Nucl. Part. Sci. **57** 205
- [6] van Hees H *et al* 2006 Phys. Rev. C **73** 034913
- [7] Tripathy S *et al* 2016 Eur. Phys. J. A **52** 289
- [8] Tripathy S *et al* 2017 Eur. Phys. J. A **53** 99
- [9] Florkowski W *et al* 2016 Phys. Rev. C **93** 064903
- [10] Tsallis C 1988 J. Stat. Phys. **52** 479
- [11] Schnedermann E *et al* 1993 Phys. Rev. C **48** 2462
- [12] Rybczynski M *et al* 2012 J. Phys. G: Nucl. Part. Phys. **39** 095004
- [13] Wilk G and Wlodarczyk Z 2000 Phys. Rev. Lett. **84** 2770
- [14] Cleymans J and Worku D 2012 J. Phys. G: Nucl. Part. Phys. **39** 025006
- [15] Cleymans J *et al* 2013 Phys. Lett. B **723** 351354
- [16] Azmi M D and Cleymans J 2014 J. Phys. G: Nucl. Part. Phys. **41** 065001
- [17] Azmi M D and Cleymans J 2015 Eur. Phys. J. C **75** 430
- [18] Marques L, Cleymans J and Deppman A 2015 Phys. Rev. D **91** 054025
- [19] Khuntia A *et al* 2017 Eur. Phys. J. A **53** 103
- [20] Adams J *et al* (STAR Collaboration) 2006 Phys. Lett. B **637** 161169
- [21] Adare A *et al* (PHENIX Collaboration) 2011 Phys. Rev. C **83** 024909
- [22] Chatrchyan S *et al* (ALICE collaboration) 2014 Eur. Phys. J. C **74** 2847
- [23] Azmi M D and Cleymans J 2014 Acta Phys. Pol. B Proc. Suppl. **7**, 9-16
- [24] Zheng H and Zhu L 2015 Adv. in High Energy Phys. **2015** 180491
- [25] Adam J *et al* (ALICE Collaboration) 2016 Phys. Rev. C **93** 034913
- [26] Abelev B *et al* (ALICE Collaboration) 2017 Phys. Rev. C **95** 064606

- [27] Abelev B *et al* (ALICE Collaboration) 2013 Phys. Rev. Lett. **111** 222301
- [28] Hanratty L D 2014 CERN-THESIS-2014-103
- [29] Abelev B *et al* (ALICE Collaboration) 2013 Phys. Rev. C **88** 044909
- [30] Acharya S *et al* (ALICE Collaboration) 2019 arXiv:1910.07678
- [31] Adam J *et al* (ALICE Collaboration) 2016 Phys. Lett. B **760** 720-735
- [32] Adam J *et al* (ALICE Collaboration) 2015 Phys. Rev. C **91** 064905
- [33] Adam J *et al* (ALICE Collaboration) 2016 Eur. Phys. J. C **76** 245
- [34] Abelev B *et al* (ALICE Collaboration) 2014 Phys. Lett. B **728** 25-38
- [35] Adam J *et al* (ALICE Collaboration) 2016 Phys. Lett. B **758** 389-401
- [36] Abelev B *et al* (ALICE Collaboration) 2013 Phys. Rev. C **88** 044910
- [37] Abelev B *et al* (ALICE Collaboration) 2014 Phys. Lett. B **736** 196-207
- [38] Acharya S *et al* (ALICE Collaboration) 2019 Phys. Lett. B **793** 420-432